Available online at www.sciencedirect.com
SCIENCE DIRECT®
Marine Geology 201 (2003) 133–146
MARINE GEOLOGY
INTERNATIONAL JOURNAL OF MARINE GEOLOGY, GEOCHEMISTRY AND GEOPHYSICS
www.elsevier.com/locate/margeo

Clay mineral assemblages in the northern South China Sea: implications for East Asian monsoon evolution over the past 2 million years

Zhifei Liu [a,*], Alain Trentesaux [b], Steven C. Clemens [c], Christophe Colin [d], Pinxian Wang [a], Baoqi Huang [a], Sébastien Boulay [d]

[a] *Laboratory of Marine Geology, Tongji University, Shanghai 200092, PR China*
[b] *Laboratoire Processus et Bilans des Domaines Sédimentaires, UMR PBDS CNRS, Université de Lille I, 59655 Villeneuve d'Ascq, France*
[c] *Department of Geological Sciences, Brown University, 324 Brook Street, Box 1846, Providence, RI 02912, USA*
[d] *Laboratoire de Géochimie des Roches Sédimentaires, FRE 2566 Orsayterre, BAT. 504, Université de Paris XI, 91405 Orsay, France*

Accepted 19 June 2003

Abstract

Clay mineral assemblages at ODP Site 1146 in the northern South China Sea are used to investigate sediment source and transport processes and to evaluate the evolution of the East Asian monsoon over the past 2 Myr. Clay minerals consist mainly of illite (22–43%) and smectite (12–48%), with associated chlorite (10–30%), kaolinite (2–18%), and random mixed-layer clays (5–22%). Hydrodynamic and mineralogical studies indicate that illite and chlorite sources include Taiwan and the Yangtze River, that smectite and mixed-layer clays originate predominantly from Luzon and Indonesia, and that kaolinite is primarily derived from the Pearl River. Mineral assemblages indicate strong glacial–interglacial cyclicity, with high illite, chlorite, and kaolinite content during glacials and high smectite and mixed-layer clay content during interglacials. During interglacials, summer enhanced monsoon (southwesterly) currents transport more smectite and mixed-layer clays to Site 1146 whereas during glacials, enhanced winter monsoon (northerly) currents transport more illite and chlorite from Taiwan and the Yangtze River. The ratio (smectite+mixed layers)/(illite+chlorite) was adopted as a proxy for East Asian monsoon variability. Higher ratios indicate strengthened summer-monsoon winds and weakened winter-monsoon winds during interglacials. In contrast, lower ratios indicate a strongly intensified winter monsoon and weakened summer monsoon during glacials. Spectral analysis indicates the mineral ratio was dominantly forced by monsoon variability prior to the development of large-scale glaciation at 1.2 Myr and by both monsoon variability and the effects of changing sea level in the interval 1.2 Myr to present.

Keywords: clay minerals; East Asian monsoon; Pleistocene; South China Sea; ODP Leg 184

* Corresponding author. Tel.: +86-21-6598-4877; Fax: +86-21-6598-8808.
E-mail address: lzhifei@online.sh.cn (Z. Liu).

0025-3227/03/$ – see front matter © 2003 Elsevier B.V. All rights reserved.
doi:10.1016/S0025-3227(03)00213-5

1. Introduction

1.1. East Asian monsoon climate and the South China Sea (SCS)

East Asian monsoon circulation is driven by differential heating between the WPWP (western Pacific warm pool) and the Asian continent. Seasonally reversing summer- and winter-monsoon winds drive seasonal precipitation and runoff regimes which determine, in part, the soil and vegetation characteristics of eastern Asia (Webster, 1994; Ding et al., 1998; Wang et al., 1999). The East Asian winter monsoon is characterized by continental cooling and the development of high pressure over northern Asia, resulting in northeast winds across the SCS (Fig. 1a). In contrast, the summer monsoon is characterized by continental heating, the development of low pressure over central China, and moderate (5 m/s) southerly winds that bring high precipitation to southern and eastern Asia driving southwesterly surface currents in the SCS (Fig. 1a). Thus, the SCS is well located to record short- and long-term paleoceanographic responses to both winter- and summer-monsoons circulation (Wang et al., 1999, 2000).

Many previous studies have addressed East Asian monsoon variability from the Late Pleistocene to the Holocene using both terrestrial and marine sediment records. These studies indicate that the Holocene and other interglacial periods were characterized by strengthened summer-monsoon and weakened winter-monsoon winds (Wang et al., 1999; Jian et al., 2001), leading to enhanced soil formation as documented in Chinese loess profiles (Kukla et al., 1988; Banerjee, 1995; Porter and An, 1995). In contrast, intensified winter-monsoon and weakened summer-monsoon circulation characterized glacial periods (Huang et al., 1997; Wang et al., 1999), leading to enhanced continental aridity and loess transport (Ding et al., 1998). Dry phases have also been linked to short-term Heinrich events and to the Younger Dryas, as observed in the Sulu Sea (Kudrass et al., 1991; Garidel-Thoron et al., 2001) and the SCS (Wang et al., 1999). The long-term history of the past 6 Myr obtained from magnetic susceptibility and aeolian grain size (Sun et al., 1998) and aeolian flux in the North Pacific (Rea et al., 1998) identified continued strengthening of the East Asian winter monsoon since 2.6 Ma. (Xiao and An, 1999; An et al., 2001). These studies were mainly based on species distribution of flora and fauna, geochemistry, and physical properties such as sedimentation rate and grain size. Clay mineralogical records from the SCS have not been widely reported. This study as well as Tamburini et al. (2003) is among the first time series records from the SCS.

1.2. Previous studies on surface sediment mineralogy

The worldwide distribution of clay minerals was examined by Griffin et al. (1968) and Rateev et al. (1969), but did not include the SCS. A few studies have been published on the clay mineral composition of surface sediments in the SCS (Chen, 1978; Clift et al., 2002). Here we use data from Chen (1978) as well as unpublished data obtained from other Chinese colleagues to compile a map of clay mineral composition for SCS surface sediments. From this we infer source

Table 1
Average clay compositions for clay mineral provinces in the SCS and early Holocene sediments at ODP Site 1146

Clay mineral	Province						ODP1146 E. Holocene
	A	B	C	D	E	F	
Kaolinite	6	12	15	20	50	20	10
Chlorite	25	21	20	19	25	23	22
Illite	65	55	42	31	20	47	38
Smectite+mixed layers	4	12	23	30	5	10	30

Data of province E after Chen and Tan (1991); others after Chen (1978); province D resulted from a combination of provinces D and E of Chen (1978).

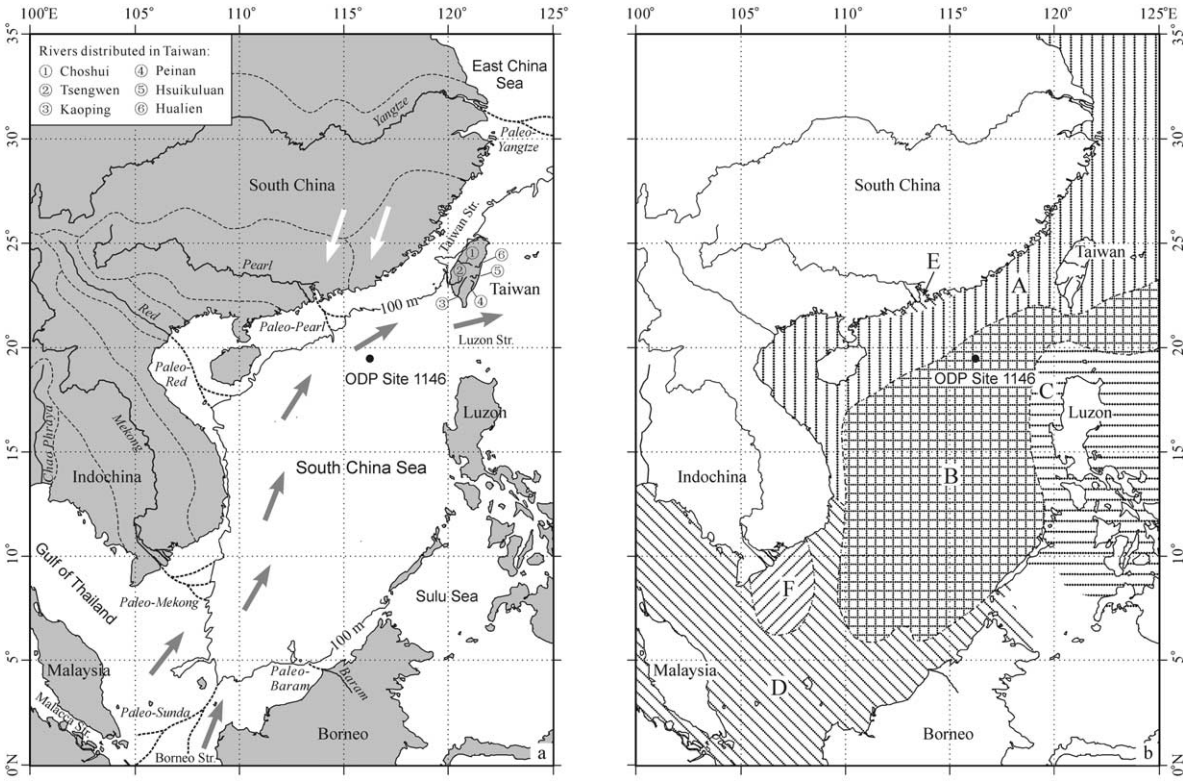

Fig. 1. (a) Major drainage systems surrounding the SCS (South China Sea) and the location of ODP Site 1146. Dashed lines in the Asian continent outline major drainage basins in South China and Indochina. Six major rivers in Taiwan are labeled. Present 100-m isobath shows approximate position of the coastline during glacial low sea level. Major rivers on the emerged glacial shelf are indicated as paleo-rivers as adapted from Wang et al. (1999) and Hiscott (2001). Gray arrows show modern surface currents during summer monsoon and white arrows during winter monsoon. (b) Clay mineral provinces for modern surface sediments throughout SCS, indicating that the provenance-controlled patterns of clay mineral distribution. Data of province E after Chen and Tan (1991); others after Chen (1978).

and transport paths in an effort to interpret downcore variability in clay mineral assemblages and ratios.

The surface distribution (modified after Chen, 1978) can be divided into six clay mineral provinces (Fig. 1b, Table 1). Province A, dominated by illite and chlorite, includes the northern shelf of the SCS, the Taiwan Strait, and the East China Sea, but not the inner estuary of the Pearl River (Fig. 1b). The illite content increases southward from about 65% at the Yangtze River estuary (Guo et al., 1995; Wang, Y. et al., 1995) to 73% at the northeastern Taiwan Strait, and 84% at the southwestern Taiwan Strait (You et al., 1993). The province has an average illite content of 65% and chlorite of 25% (Table 1). Province B includes the central part of the SCS and extends northeastward through the Luzon Strait. Relative to province A, illite and chlorite are reduced by 5–10% whereas smectite (and mixed layers) and kaolinite increase by 6–8%. In northern parts of province B, illite content reaches 60–65% (He, 1992). In province C, surrounding the Luzon islands, smectite increases to 23%, twice the amount in province B. Province D covers most of the Sunda shelf and extends to the Gulf of Thailand and the Malacca Strait. Smectite becomes very prominent in this province, ranging from 20% to 50%, with an average of 30% (Chen, 1978). Coastal province E, including the bay and inner estuary of the Pearl River, is characterized by high kaolinite (50%) which rapidly decreases slope-ward (Chen

and Tan, 1991). Province F, the Mekong River estuary, is relatively rich in illite and chlorite (47% and 23% respectively). The kaolinite content in provinces C, D, and F averages about 20%, but reaches 50% in the Malacca Strait (Chen, 1978).

The surface clay mineral composition in the SCS does not appear to correlate with lithological variation, environmental energy conditions, or diagenetic state (Chen, 1978). The primary control on the variation of mineral assemblages in surface sediments, therefore, is provenance (Chen, 1978; He, 1989; Tan and Wang, 1992). Two main source areas with markedly different geological characteristics contribute sediment to the SCS. The northern source is mainly the Asian continent and Taiwan while the southern source consists of islands or volcanic arcs that bound the SCS to the east and south. Weathering products from the Asian continent are transported to the SCS chiefly by rivers, including the Yangtze, Mekong, and Red rivers which discharge 768×10^6 tons of sediments annually (Table 2). About 30% of the Yangtze sediment discharge is observed to be transported southward (Milliman et al., 1985), in nearshore currents along the China coast (Chen, 1978). All three rivers originate in the Tibetan Plateau flowing through tectonically active areas of central China or the Indochina Peninsula characterized by strong physical weathering regimes. Suspended sediments in these rivers are characterized by abundant illite and chlorite and rather scarce kaolinite and smectite in the clay fraction (Wang, Y. et al., 1995; Nguyen and Egashira, 2000) and are primary sources for provinces A and F. However, the Pearl River, draining sub-tropical, vegetated South China, flows through kaolinite-developed soils in Guangdong Province (Xu et al., 1999) and contributes kaolinite to the SCS via province E (Chen and Tan, 1991).

Six major rivers from Taiwan (Fig. 1a) contribute 185×10^6 tons of sediments annually to the SCS (Table 2; Milliman and Meade, 1983). The suspended sediments in clay fractions surrounding Taiwan mainly consist of illite and chlorite (Chen, 1978; Dorsey et al., 1988). Clay mineral assemblages in the sea surrounding the Luzon islands and in the southwestern SCS are characterized by a high content of smectite and kaolinite (Fig. 1b, Table 1). The origin of smectite is generally related to volcanic activity or the alteration of volcanic materials by hydrothermal and weathering processes (Chamley, 1989). The abundance of smectite surrounding the Luzon islands is similar that of volcaniclastic sediments (Shi et al., 1995) suggesting that volcanoes are principal sources for smectite in the surrounding seas (province C). Other river inputs to the southwest SCS include the Baram from northwest Borneo and the Chao Phraya from west Indochina, with a combined annual sediment discharge of 23×10^6 tons (Fig. 1a, Table 2) (Milliman and Syvitski, 1992; Hiscott, 2001). Their clay compositions are poorly known and are considered of minor importance

Table 2
Drainage area, water and suspended sediment discharges for major rivers surrounding SCS

River	Drainage area ($\times10^6$ km^2)	Water discharge (km^3/yr)	Suspended sediment discharge ($\times10^6$ tons/yr)	Data source
Yangtze River	1.94	900	478	Milliman and Meade (1983)
Mekong River	0.79	470	160	
Red River	0.12	123	130	
Pearl River	0.44	302	69	
Choshui (Taiwan)	0.003	6	66	
Kaoping (Taiwan)	0.003	9	39	
Tsengwen (Taiwan)	0.001	2	28	
Hualien (Taiwan)	0.002	4	19	
Peinan (Taiwan)	0.002	4	17	
Hsiukuluan (Taiwan)	0.002	4	16	
Baram (Malaysia)	0.0192	46	12	Hiscott (2001)
Chao Phraya (Thailand)	0.16	30	11	Milliman and Syvitski (1992)

given the small annual discharge. The Indonesian islands, south of the Sunda shelf, provides 20–40% smectite and 30–40% kaolinite to the Java Sea (Gingele et al., 2001) suggesting that they are also mineral sources for province D. The central SCS (province B) is considered as a transitional area in that it contains a mixture of all mineral compositions from surrounding continents and islands. Therefore, downcore clay mineral assemblages in province B reflect relative contributions from different sources according to changes in source area weathering and transport paths, which are, in turn, driven by monsoon circulation. Here we perform clay mineral analyses from Ocean Drilling Program (ODP) Site 1146, which is situated in the northern part of province B (Fig. 1), to evaluate East Asian monsoon variability over the past 2 Myr.

2. Materials and methods

ODP Site 1146 is located at 19°27.40′N, 116°16.37′E, at a water depth of 2092 m, within a small rift basin on the mid-continental slope of the northern SCS (Fig. 1a). A total of 515 samples were taken at ~40-cm intervals from the upper part of holes 1146A, B, and C (1–190 mcd, meters composite). This yields a temporal resolution of about 4 kyr per sample. These sediments are composed of greenish-gray nannofossil clay.

The methodology and clay mineral data are reported in Trentesaux et al. (2003). Here we present detailed analysis and interpretation of these data relative to paleoceanographic and paleoclimatic change in the SCS. Briefly, preparation and measurement of clay mineral analysis were performed at the Laboratoire Processus et Bilans des Domaines Sédimentaire, Université de Lille I. Clay minerals were identified by X-ray diffraction (XRD) on oriented mounts of clay-sized particles (Holtzapffel, 1985). Deflocculation was accomplished by successive washing with distilled water after decarbonation with 0.2 N HCl. The particles less than 2 μm were separated by sedimentation and centrifugation. XRD diagrams were obtained using a Philips PW 1710 diffractometer with CuKα radiation and Ni filter, under a voltage of 40 kV and an intensity of 25 mA. Three XRD runs were performed, following air-drying, ethylene–glycol solvation for 12 h, and heating at 490°C for 2 h. Goniometer scans were from 2.5° to 32.5° 2θ for air-dried and glycolated conditions, and from 2.5° to 14.5° 2θ for heated conditions.

Identification of clay minerals was made mainly according to the position of the (001) series of basal reflections on the three XRD diagrams. Semi-quantitative estimates of peak areas of the basal reflections of the main clay mineral groups of smectite (17 Å), mixed-layer clays (15 Å), illite (10 Å), and kaolinite/chlorite (7 Å) were carried out on the glycolated curve (Holtzapffel, 1985) using the MacDiff software (Petschick, 2000). Kaolinite and chlorite were separated by relative proportions according to the ratios of the areas of the 3.57/3.54 Å peaks. Kaolinite/chlorite proportions were used to compute proportions of the 7 Å peak area for the respective mineral. The mixed-layer clays mainly consist of random smectite–illite and smectite–chlorite mixed layers. Smectite–illite mixed layers have small asymmetric peaks between 10 and 14 Å in the air-dried sample, while smectite–chlorite mixed layers give a plateau (or shoulder) between 10 and 14 Å in the heated sample. But they move to the area between 14 and 17 Å in the glycolated sample. These characteristic peaks of mixed-layer minerals are largely due to random interstratification of smectite with minor illite and chlorite. The clay mineral ratio, (smectite+mixed layers)/(illite+chlorite), was derived to evaluate the relative significance of clay mineral sources, serving as an indicator of the East Asian monsoon evolution.

The $\delta^{18}O$ record (0–167 mcd; *Globigerinoides ruber*, white) has a nominal 2 kyr temporal resolution and was generated at Brown University on a Finnigan MAT 252 with a Kiel III carbonate device (Clemens and Prell, 2003). Results are reported relative to the Vienna Pee Dee belemnite (VPDB) standard and have an external error of $\pm 0.10‰$. The age–depth model used in this paper was established using oxygen isotope stratigraphy, biostratigraphy, and paleomagnetism (Table 3). The last occurrence of *G. ruber* (pink) at about 120 kyr (Thompson et al., 1979) appeared

at depth of 25.95 mcd (Huang, 2002). Several paleomagnetic boundaries, including Brunhes/Matuyama, Upper Jaramillo, and Lower Jaramillo, occurred at 115.50, 132.50, and 137.90 mcd, respectively (Shipboard Scientific Party, 2000). The age–depth model in the lower part of the core (185.5–190 mcd) is based on $\delta^{18}O$ stratigraphy obtained from *C. wuellerstorfi*, measured at an average of 40-cm intervals on a Finnigan MAT 252 mass spectrometer with a Kiel carbonate device at Laboratory of Marine Geology, Tongji University. These data (VPDB) have an external error of ±0.07‰ (Huang, 2002).

3. Results

Illite (22–43%) and smectite (12–48%) dominant during most of Quaternary (10–1988 kyr before present) at Site 1146 with a combined total of more than 60% (Fig. 2). Clay minerals in less abundance include chlorite (10–30%), kaolinite

Table 3
Data of age–depth model for Site 1146 in the northern SCS

Event	Depth (mcd)	Age (kyr)	Data source
Oxygen isotope	0.00	8	Clemens and Prell (2003)
	6.00	21	
	16.00	65	
G. ruber (pink), LO	25.95	120	Huang (2002)
Oxygen isotope	27.00	135	Clemens and Prell (2003)
	32.27	180	
	41.47	228	
	47.00	249	
	56.00	299	
	60.00	343	
	66.57	400	
	71.22	415	
	77.00	472	
	86.19	540	
	93.80	610	
	95.70	635	
	102.19	660	
	107.46	716	
	111.23	755	
	113.80	770	
Brunhes/Matuyama, PM	115.50	780	Shipboard Scientific Party (2000)
Oxygen isotope	116.60	800	Clemens and Prell (2003)
	119.38	845	
	122.00	872	
	127.00	921	
Upper Jaramillo, PM	132.50	990	Shipboard Scientific Party (2000)
Lower Jaramillo, PM	137.90	1070	
Oxygen isotope	139.25	1090	Clemens and Prell (2003)
	141.00	1130	
	146.00	1190	
	150.00	1250	
	152.00	1295	
	155.00	1365	
	161.00	1445	
	163.00	1495	
Oxygen isotope	198.70	2084	Huang (2002)

LO = last occurrence; PM = paleomagnetism.

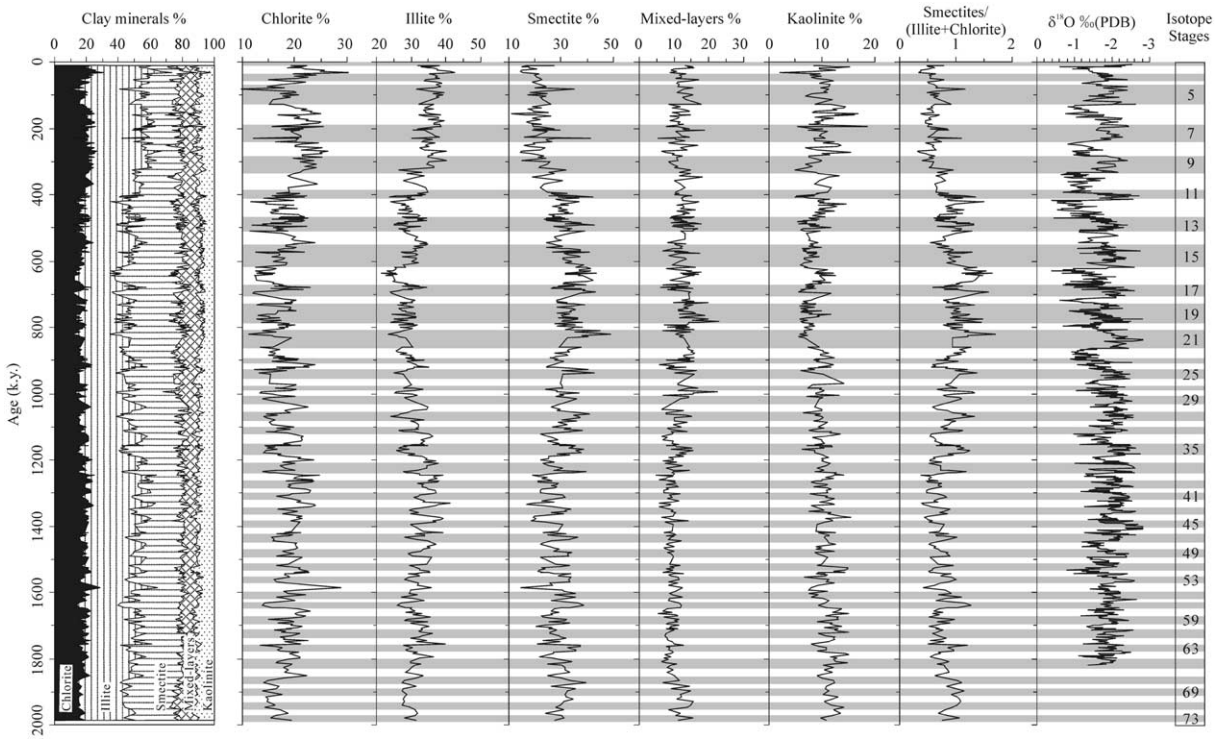

Fig. 2. Variations of clay mineral assemblages of Site 1146 over the past 2 Myr. Mixed layers mainly refer to random smectite–illite and smectite–chlorite mixed layers. Isotope stages were obtained by visually correlating $\delta^{18}O$ (Clemens and Prell, 2003) (stages 1–65) and smectites/(illite+chlorite) ratio (stages 66–73) to $\delta^{18}O$ records of ODP Site 677 (Shackleton et al., 1990).

(2–18%), and random mixed layers (5–22%). Lesser amounts of quartz and feldspar also occur in the clay fraction. Core top samples from Site 1146 have not been radiometrically dated although isotope stratigraphy suggests they are early Holocene in age. These samples consist mainly of illite (38%) and smectite (and mixed layers) (30%), with associated chlorite (22%) and kaolinite (10%), indicating higher smectite (and mixed layers) and lower illite content relative to surface sediments in province B (Table 1). Such differences can result from different climate conditions between early Holocene and present or from differences in the semi-quantitative analytical techniques applied by laboratories generating the two data sets.

The clay mineral concentrations indicate the strong glacial–interglacial cyclicity throughout the past 2 Myr (Fig. 2). Generally, illite and chlorite show a similar pattern of cyclic change, with high values during glacials, when illite reaches 35–43% and chlorite 20–30%. On the contrary, smectite has a range of over 30% with high values during interglacials. Relatively high values of smectite occur in the interval 1200–400 kyr (Fig. 2). Kaolinite has a mean of ~12% with high values during most glacial cycles (Fig. 2). Unlike other clay minerals, mixed-layer clays and smectite have similar variability but no obvious relation to changes in ice volume ($\delta^{18}O$). Considering that the mixed-layer clays mainly originate from random interstratification of smectite with minor illite and chlorite and that smectite and mixed-layer clays have similar variability, we group both as 'smectites' = (smectite+mixed layers) for the purposes of this study.

The clay mineral ratio, smectites/(illite+chlorite) varies from 0.3 to 1.8, with an average of 0.9. The ratio mean reaches a maximum in the interval 1200–400 kyr Overall, the variability is

strongly correlated with the oxygen isotope record (higher values during interglacials) prior to about 1000 kyr, moderately correlated from 1000 kyr to 400 kyr, and poor correlation in the uppermost part of the record (Fig. 2).

4. Discussion

4.1. Clay mineral sources

The paleoclimatic interpretation of clay mineral data requires knowledge of the potential source areas as well as the mode and strength of transport processes (Diekmann et al., 1996; Gingele et al., 1998). As previously described, Site 1146 is located in the northern part of clay mineral province B (Fig. 1b), which contains a mixture of minerals from surrounding continents and islands. Illite and chlorite at Site 1146 are mainly derived from the Asian continent via the Yangtze River, as well as from Taiwan, through province A (Fig. 1b) with less important contributions by aeolian input from northern Asia.

Smectites at Site 1146 likely come from the Luzon islands in the east and the Indonesian islands in the south. These areas, characterized by the common occurrence of volcaniclastic sediments, provide abundant smectite to provinces C and D, respectively (Shi et al., 1995; Gingele et al., 2001). The source of kaolinite at Site 1146 is more complicated, because South China (Pearl River) and the Luzon and Indonesian islands all contribute kaolinite to the SCS (Table 1). Relative contributions from these sources vary with transport paths (ocean currents) and paleoclimate conditions.

During interglacial periods, the coastline is approximately similar to present and southwesterly surface currents driven by summer-monsoon winds prevailed in most areas of the SCS (Wang et al., 1995; Huang et al., 1997) (Fig. 3a). These currents presumably transport abundant smectites from the Indonesian islands through the Borneo Strait in the south and from the Luzon islands in the east to the position of Site 1146. Because decreased illite and kaolinite content does not follow changes in smectite during interglacials, illite and chlorite from the Red and Mekong rivers and kaolinite from Luzon and Indonesia are considered of minor importance in terms of contribution to Site 1146. Instead, illite and chlorite likely come from Taiwan and the Yangtze River through the Taiwan Strait. Kaolinite, less than 10% during interglacials, is thought to originate from the Pearl River, which carries an abundance of this mineral in the modern (Chen and Tan, 1991). During glacial periods, the coastline follows the approximate position of the present-day 100-m isobath; the Borneo Strait, the Gulf of Thailand, and the Taiwan Strait were closed (Fig. 3b). Counter-clockwise surface circulation driven by strengthened winter-monsoon winds dominated the semi-enclosed SCS (Wang et al., 1995). The Paleo-Yangtze River estuary shifted southeastward about 3500 km closer to the SCS. However, sediments from this paleo-river system were likely contained within the Okinawa Trough, offshore northeast Taiwan. Thus, we suggest that Taiwan is the most important source of illite and chlorite to Site 1146 during glacial intervals with the Yangtze River of lesser importance. A recent study on geochemical analysis of the past 1.05 Myr for the provenance of ODP Site 1144, which is situated to the northeast of Site 1146, suggested Taiwan as the main source area as well (Shao et al., 2001). The exposed shelf of the northern SCS during glacial low stands as well as aeolian transport from northern Asia may also contribute illite and chlorite. Kaolinite is likely sourced by the Paleo-Pearl River, whose estuary was shifted closer to Site 1146 and its content shows higher values during glacials. Smectites likely originate from the Luzon islands in the east and the exposed Sunda shelf in the south, delivered by the Paleo-Sunda River and transported to Site 1146 by counter-clockwise surface currents during glacials.

4.2. Mineralogical indicator of East Asian monsoon evolution

Variations in the downcore clay mineral distribution in deep-sea sediments have been interpreted in terms of changes in the climatic conditions prevailing in the continental source area (Chamley, 1967, 1989; Clayton et al., 1999; Colin

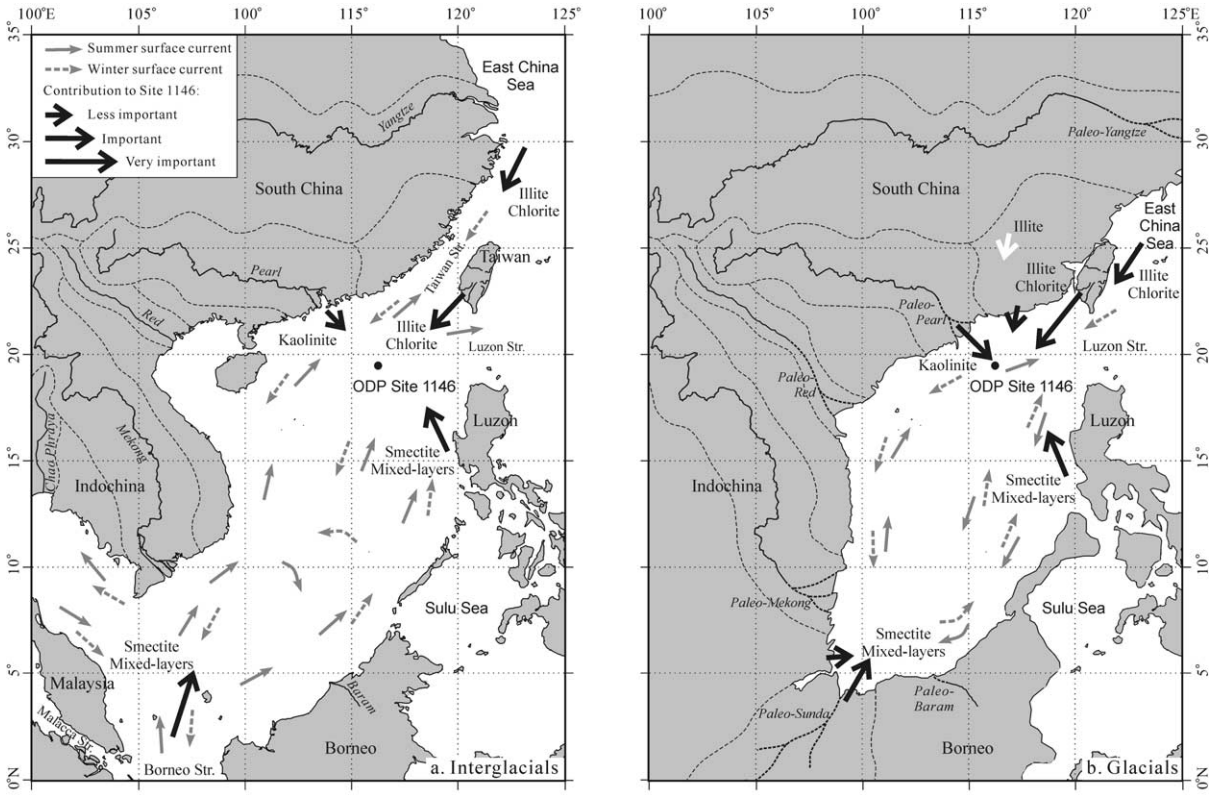

Fig. 3. Source analysis of clay minerals at Site 1146. (a) Interglacial periods: the coastline is approximately the present one. Illite and chlorite mainly come from Taiwan and the Yangtze River through the Taiwan Strait. Smectites are mainly transported in from the Indonesian islands through the Borneo Strait and also from the Luzon islands. Kaolinite is mainly brought in from the Pearl River. (b) Glacial periods: the coastline is moved to the approximate position of present 100-m isobath; the Borneo Strait, Gulf of Thailand, and the Taiwan Strait were closed. Illite and chlorite mainly came from Taiwan, as well as the Paleo-Yangtze River through via southward coastal currents. The exposed shelf of the northern SCS and aeolian transport from northern Asia provide less important contributions of illite and chlorite. Smectites mainly came from the Luzon islands in the east and the exposed Sunda shelf in the south, transported by the Paleo-Sunda River. The Paleo-Pearl River contributed most of the kaolinite to Site 1146. Data for surface ocean currents after Wang et al. (1995).

et al., 1999; Foucault and Mélières, 2000). However, recent investigations (Thiry, 2000) suggest that changes in marine clay mineral assemblages do not uniquely reflect changes in weathering conditions of the terrigenous source, because weathering profiles develop over long periods of time. Concerning our study of Site 1146 in the northern SCS, illite and chlorite mainly come from Taiwan and the Yangtze River (Fig. 3), which drain vast source areas with a wide variety of environmental conditions. In particular during glacial periods, when values of illite and chlorite are highest, additional sources include the exposed shelf of the northern SCS as well as aeolian transport from northern Asia. Kaolinite carried by the Pearl River primarily originates from weathering profiles that prevail in sub-tropical areas during interglacials. The higher kaolinite content during glacials may also reflect the overall increase in terrigenous input during sea level low stands (Wang et al., 1995). Smectites, provided mainly by the Luzon and Indonesian islands, could be formed preferentially from volcanic rocks, regardless of climate conditions, if there is sufficient water to allow hydrolytic processes (Chamley, 1989). Consequently, the clay mineral assemblages at Site 1146 were not only controlled by contemporary climates of sources surrounding the SCS but

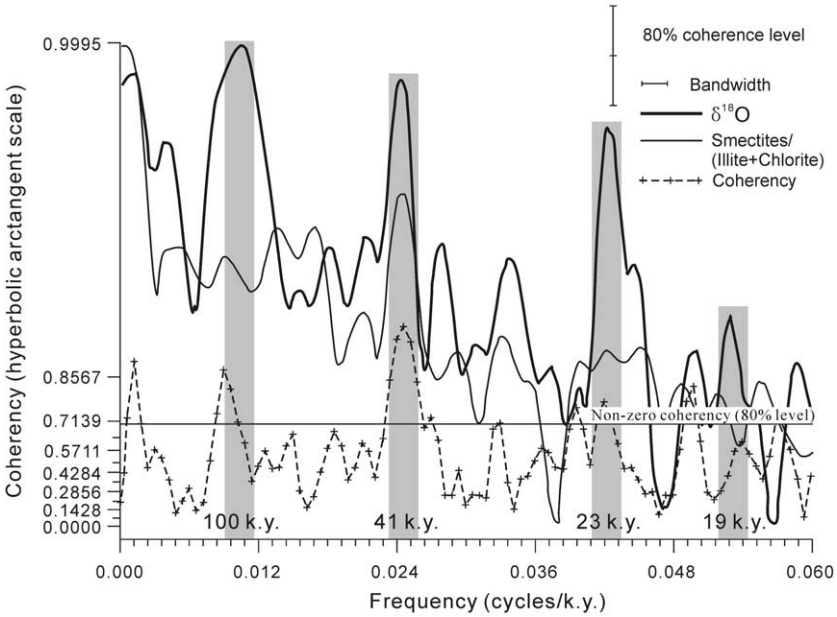

Fig. 4. Cross-spectral analysis between the clay mineral ratio of smectites/(illite+chlorite) and planktonic $\delta^{18}O$ at ODP Site 1146. $N = 900$, interpolation = 2 kyr, 300 lags. The solid horizontal line indicates 80% non-zero coherency level. Eccentricity (100 kyr), obliquity (41 kyr), and precession (23 and 19 kyr) bands are shaded.

also by changing strength of the transport processes. As such, clay mineral records at Site 1146 can be used to trace summer- and winter-monsoon variability, which controls the intensity of the surface ocean currents in the SCS. Similar approaches have been used by other investigators on ocean-wide (Petschick et al., 1996) as well as regional scales (Gingele, 1996; Gingele et al., 2001).

Generally, multiple sources and transport processes as well as the dilution of individual clay minerals make it difficult to assign changes in the downcore record of any one component to a change in a specific paleoclimatic factor (Gingele et al., 1998). The comparison of two components by their ratio offers the advantage of reducing dilution effects by other components.

In general, illite and chlorite content increased during glacials and decreases during interglacials, whereas smectite content varies in opposition, increasing during interglacials and decreasing during glacials (Fig. 2). Kaolinite generally follows illite and chlorite with high values during glacials. Here we adopt the ratio of smectites/(illite+chlorite) as a mineralogical indicator of East Asian monsoon evolution in the northern SCS. The relatively high ratio during interglacials reflects strengthened summer-monsoon and weakened winter-monsoon winds; in contrast, the lower ratio during glacials indicates a strongly intensified winter monsoon and weakened summer monsoon, as suggested by previous studies using micropaleonotological proxies (Huang et al., 1997; Wang et al., 1999; Jian et al., 2001).

In the interval 1200–400 kyr, the ratio indicates relatively higher values. The smectites/(illite+chlorite) ratio is generally larger than 1.0 during interglacials and smaller than 1.0 during glacials (Fig. 2). This suggests reduced seasonality due to strengthened interglacial summer-monsoon winds which enhance southwesterly surface ocean currents bringing in increased smectites from southern and eastern sources. During other intervals (2000–1200 and 400–0 kyr) the ratio generally is less than 1.0 for both interglacials and glacials, suggesting the East Asian winter monsoon is dominant during most of the Pleistocene as indicated by the Chinese loess records spanning the

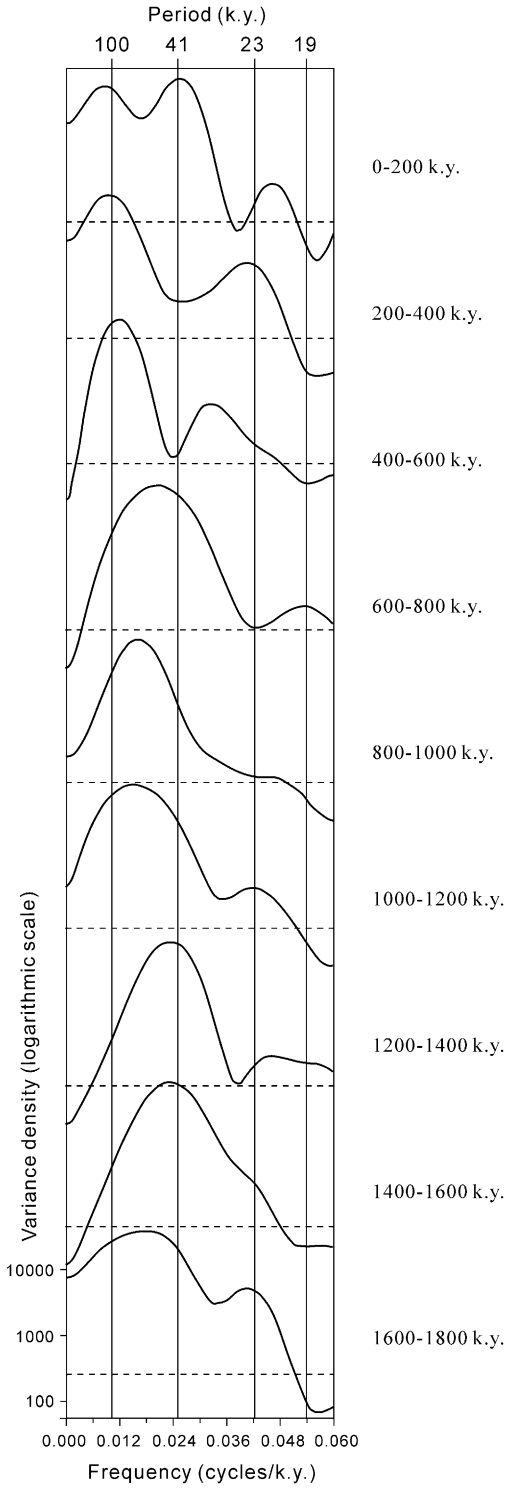

past 2.6 Ma (An et al., 2001). These patterns are also were observed in loess–paleosol records in northern Asia as increased contrast between the East Asian summer and winter monsoons beginning about 1200 kyr and a strongly developed summer- and winter-monsoon circulation since about 550 kyr (Xiao and An, 1999).

4.3. Spectral analysis of the mineralogical ratio

Cross-spectral analysis between the clay mineral ratio of smectites/(illite+chlorite) and planktonic $\delta^{18}O$ at Site 1146 is used to assess the relationship between the two proxy climate indicators in the frequency domain (Fig. 4). Over the past 1800 kyr, the planktonic $\delta^{18}O$ record indicates strong concentrations of variance at all orbital periods (100, 41, and 23 kyr). In contrast, the mineral ratio proxy indicates a strong concentration of variance only in the 41-kyr obliquity band, where coherence with $\delta^{18}O$ is above the 90% confidence interval. This indicates that 41-kyr cycles dominated the mineral ratio over much of the past 1.8 Myr. Evolutionary spectra (Fig. 5) of the mineralogical indicator indicate particularly strong 41-kyr cycles in the intervals from 1.6 to 1.2 Myr, prior to the development of the 100-kyr ice age cycles. During this interval, the ratio was likely forced predominantly by monsoon-related transport processes. From 1200 to 600 kyr the dominant spectral peak is between the 100-kyr eccentricity and the 41-kyr obliquity periods, possibly responding to both monsoon forcing and sea level changes; beating between a 100-kyr sea level period and a 41-kyr monsoon period will yield a 70-kyr beat period. In the last 600 kyr the 100-kyr period dominated, suggesting that the sea level changes contributed to variability in the mineral ratio indicator during this interval.

Fig. 5. Evolutionary spectra for the clay mineral ratio of smectites/(illite+chlorite) at ODP Site 1143. Each successive spectrum is an offset of 200 kyr. Spectra were generated from data interpolated to a constant 2-kyr interval, 30 lags, $N = 100$ samples. Dashed horizontal line indicates 80% non-zero coherency intervals.

5. Conclusions

Variations of clay mineral assemblages at ODP Site 1146 in the northern SCS have been studied to investigate sources and transport processes of clay minerals, and to deduce the evolution of East Asian monsoon over the past 2 Myr. From this study, we draw the following conclusions:

(1) The clay mineral assemblages mainly consist of illite (22–43%), smectite (12–48%), chlorite (10–30%), kaolinite (2–18%), and random mixed layers (5–22%). Generally, illite and chlorite content increased during glacials reaching as much as 35–43% for illite and 20–30% for chlorite, whereas smectite and mixed-layer content shows high values during interglacials. The kaolinite content increased during glacials for most of the glacial–interglacial cycles.

(2) For both interglacial and glacial periods, illite and chlorite at Site 1146 mainly come from Taiwan and the Yangtze River on the Asian continent; smectite and mixed-layer clays basically originate from the Luzon and Indonesian islands; kaolinite is primarily sourced by the Pearl River in South China. During interglacials, prevailing southwesterly surface currents driven by enhanced summer-monsoon winds transport increased smectite and mixed layers to Site 1146 whereas during glacials, southward nearshore currents driven by enhanced winter-monsoon winds transported more illite and chlorite from the Yangtze River to Site 1146 through the Luzon Strait. Glacial transport of illite and chlorite from Taiwan is important as well. Fluctuations of kaolinite were due to shifts in the proximity of the Pearl River estuary relative to Site 1146 during sea level low stands.

(3) The smectites/(illite+chlorite) ratio was adopted as a proxy for East Asian monsoon variability. Higher ratios indicate strengthened summer-monsoon winds and weakened winter-monsoon winds during interglacials. In contrast, lower ratios indicate a strongly intensified winter monsoon and weakened summer monsoon during glacials. Generally higher mean values indicate enhanced seasonality in the interval 1200 to 400 kyr. Spectral analysis of the mineral ratio indicates the strong orbital-scale cyclicity throughout the past 2 Myr with a particularly strong 41-kyr component prior to the development of large-scale glaciation at 1.2 Myr. Evolutionary spectral analysis suggests that the mineral ratio was dominantly forced by monsoon variability prior to the development of large-scale glaciation at 1.2 Myr and by both monsoon variability and the effects of changing sea level in the interval 1.2 Myr to present.

Acknowledgements

We are thankful to Philippe Récourt and Deny Malengros for their technical assistance in the laboratory and to Prof. H. Chamley for helpful comments. We specially thank the Marine Geology Editor-in-Chief, Dr. Eve Arnold, and one anonymous reviewer for their encouragement and constructive reviews that significantly helped to improve this work. All samples used in this study were provided by ODP, which is sponsored by the U.S. National Science Foundation (NSF) and participating countries under management of Joint Oceanographic Institutions (JOI), Inc. This study was supported by the French-China program (PRA T99-02), the National Key Basic Research Special Foundation Project of China (G2000078500), and the National Natural Science Foundation of China (49999560 and 40102010).

References

An, Z., Kutzbach, J.E., Prell, W.L., Porter, S.C., 2001. Evolution of Asian monsoons and phased uplift of the Himalaya-Tibetan plateau since Late Miocene times. Nature 411, 62–66.

Banerjee, S.K., 1995. Chasing the paleomonsoon over China: its magnetic record. GAS Today 5, 93–97.

Chamley, H., 1967. Possibilités d'utilisation de la crisatallinité d'un mineral argileux (illite) comme témoin climatique dans les sediments récents. C. R. Acad. Sci. Paris Sér. D 265, 184–187.

Chamley, H., 1989. Clay Sedimentology. Springer, Berlin, 623 pp.

Chen, P.-Y., 1978. Minerals in bottom sediments of the South China Sea. Geol. Soc. Am. Bull. 89, 211–222.

Chen, Y., Tan, H., 1991. Clay minerals in surface sediment of Lingdingyang Bay in the Zhujiang River Mouth (in Chinese, with English abstr.). Trop. Geogr. 11, 39–44.

Clayton, T., Pearce, R.B., Peterson, L.C., 1999. Indirect climatic control of the clay mineral composition of Quaternary sediments from the Cariaco basin, northern Venezuela (ODP Site 1002). Mar. Geol. 161, 191–206.

Clemens, S.C., Prell, W.L., 2003. Data report: preliminary oxygen and carbon isotopes from site 1146, northern South China Sea. In: Prell, W.L., Wang, P., Blum, P., Clemens, S. (Eds.), Proc. ODP Sci. Res., Vol. 184, 1–8 (online).

Clift, P., Lee, J.I., Clark, M.K., Blusztajn, J., 2002. Erosional response of South China to arc rifting and monsoonal strengthening: a record from the South China Sea. Mar. Geol. 184, 207–226.

Colin, C., Turpin, L., Bertaux, J., Desprairies, A., Kissel, C., 1999. Erosional history of the Himalayan and Burman ranges during the last two glacial-interglacial cycles. Earth Planet. Sci. Lett. 171, 647–660.

Diekmann, B., Petschick, R., Gingele, F.X., Fütterer, D.K., Abelmann, A., Gersonde, R., Brathauer, U., Mackensen, A., 1996. Clay mineral fluctuations in late Quaternary sediments of the southeastern South Atlantic: implications for past changes of deepwater advection. In: Wefer, G., Berger, W.H., Siedler, G., Webb, D. (Eds.), The South Atlantic: Present and Past Circulation. Springer, Berlin, pp. 621–644.

Ding, Z.L., Sun, J.M., Yang, S.L., Liu, T.S., 1998. Preliminary magnetostratigraphy of a thick eolian red-clay loess sequence at Lingtai, the Chinese Loess Plateau. Geophys. Res. Lett. 25, 1225–1228.

Dorsey, R.J., Buchovecky, E.J., Lundberg, N., 1988. Clay mineralogy of Pliocene-Pleistocene mudstones, eastern Taiwan: combined effects of burial diagenesis and provenance unroofing. Geology 16, 944–947.

Foucault, A., Mélières, F., 2000. Palaeoclimatic cyclicity in central Mediterranean Pliocene sediments: the mineralogical signal. Palaeogeogr. Palaeoclimatol. Palaeoecol. 158, 311–323.

Garidel-Thoron, T.d., Beaufort, L., Linsley, B.K., Dannenmann, S., 2001. Millennial-scale dynamics of the East Asian winter monsoon during the last 200, 000 years. Paleoceanography 16, 491–502.

Gingele, F.X., 1996. Holocene climatic optimum in Southwest Africa - evidence from the marine clay mineral record. Palaeogeogr. Palaeoclimatol. Palaeoecol. 122, 77–87.

Gingele, F.X., Deckker, P.D., Hillenbrand, C.-D., 2001. Clay mineral distribution in surface sediments between Indonesia and NW Australia - source and transport by ocean currents. Mar. Geol. 179, 135–146.

Gingele, F.X., Müller, P.M., Schneider, R.R., 1998. Orbital forcing of freshwater input in the Zaire Fan area - clay mineral evidence from the last 200 kyr. Palaeogeogr. Palaeoclimatol. Palaeoecol. 138, 17–26.

Griffin, J.J., Windom, H., Goldberg, E.D., 1968. The distribution of clay minerals in the world ocean. Deep-Sea Res. 15, 433–459.

Guo, Z., Yang, Z., Wang, Z., 1995. Influence of water masses on the distribution of sea-floor sediments in the Huanghai Sea and the East China Sea (in Chinese, with English abstr.). J. Ocean Uni. Qingdao 25, 75–84.

He, L., 1989. Clay minerals in the Chinese and adjacent seas (in Chinese). Sci. China Ser. B 1, 75–83.

He, L., 1992. Clay minerals in the cores from the South China Sea (in Chinese, with English abstr.). J. Ocean Uni. Qingdao 22, 73–81.

Hiscott, R.N., 2001. Depositional sequences controlled by high rates of sediment supply, sea-level variations, and growth faulting: the Quaternary Baram Delta of northwestern Borneo. Mar. Geol. 175, 67–102.

Holtzapffel, T., 1985. Les Minéraux Argileux: Préparation, Analyse Diffractométrique et Détermination. Soc. Géol. Nord Publ. 12, 136 pp.

Huang, B., 2002. Late Plio-Pleistocene Evolution of the East Asian Monsoon Recorded by Foraminiferal Fauna in the Northern South China Sea. Tongji University, Shanghai, 98 pp.

Huang, C.-Y., Liew, P.-M., Zhao, M., Chang, T.-C., Kuo, C.-M., Chen, M.-T., Wang, C.-H., Zhang, L.-F., 1997. Deep sea and lake records of the Southeast Asian paleomonsoons for the last 25 thousand years. Earth Planet. Sci. Lett. 146, 59–72.

Jian, Z., Huang, B., Kuhnt, W., Lin, H.-L., 2001. Late Quaternary upwelling intensity and East Asian Monsoon forcing in the South China Sea. Quat. Res. 55, 363–370.

Kudrass, H.R., Erlenkeuser, H., Vollbrecht, R., Weiss, W., 1991. Global nature of the Younger Dryas cooling event inferred from oxygen isotope data from Sulu Sea cores. Nature 349, 406–409.

Kukla, G., Heller, F., Ming, X.L., Chun, X.-T., Liu, T.-S., An, Z.-S., 1988. Pleistocene climates in China dated by magnetic susceptibility. Geology 16, 811–814.

Milliman, J.D., Meade, R.H., 1983. World-wide delivery of river sediment to the oceans. J. Geol. 91, 1–21.

Milliman, J.D., Shen, H.-T., Yang, Z.-S., Meade, R.H., 1985. Transport and deposition of river sediment in the Changjiang estuary and adjacent continental shelf. Cont. Shelf Res. 4, 37–45.

Milliman, J.D., Syvitski, J.P.M., 1992. Geomorphic/tectonic control of sediment discharge to the ocean: the importance of small mountainous rivers. J. Geol. 100, 525–544.

Nguyen, H.U., Egashira, K., 2000. Clay mineralogical composition of some fluvisols in Vietnam. Clay Sci. 11, 205–217.

Petschick, R., 2000. MacDiff 4.2.2. Available at: http://server-mac.geologie.un-frankfurt.de/Rainer.html.

Petschick, R., Kuhn, G., Gingele, F., 1996. Clay mineral distribution in surface sediments of the South Atlantic: sources, transport, and relation to oceanography. Mar. Geol. 130, 203–229.

Porter, S.C., An, Z., 1995. Correlation between climate events in the North Atlantic and China during the last glaciation. Nature 375, 305–308.

Rateev, M.A., Gorbunova, Z.N., Lisitzyn, A.P., Nosov, G.L., 1969. The distribution of clay minerals in the oceans. Sedimentology 13, 21–43.

Rea, D.K., Snoeck, H., Joseph, L.H., 1998. Late Cenozoic eolian deposition in the North Pacific Asian drying, Tibetan

uplift, and cooling of the Northern Hemisphere. Paleoceanography 13, 215–224.

Shackleton, N.J., Berger, A., Peltier, W.R., 1990. An alternative astronomical calibration of the lower Pleistocene timescale based on ODP Site 677. Trans. R. Soc. Edinb. Earth Sci. 81, 251–261.

Shao, L., Li, X., Wei, G., Liu, Y., Fang, D., 2001. Provenance of a prominent sediment drift on the northern slope of the South China Sea. Sci. China Ser. D 44, 919–925.

Shi, X., Chen, L., Li, K., Wang, Z., 1995. Study on mineralogeny of the clay sediment in the west of Philippine Sea (in Chinese, with English abstr.). Mar. Geol. Quat. Geol. 15, 61–72.

Shipboard Scientific Party, 2000. Site 1146. In: Wang, P., Prell, W.L., Blum, P., et al. (Eds.), Proc. ODP Init. Rep., Vol. 184 [CD-ROM]. Available from: Ocean Drilling Program, Texas AIIM University, College Station, TX 77845-9547, USA, pp. 1–101.

Sun, D.H., An, Z.S., Shaw, J., Bloemendal, J., Sun, Y.B., 1998. Magnetostratigraphy and palaeoclimatic significance of Late Tertiary Aeolian sequences in the Chinese Loess Plateau. Geophys. J. Int. 134, 207–212.

Tamburini, F., Adatte, T., Föllmi, K., Bernasconi, S.M., Steinmann, P., 2003. Investigating the history of East Asian monsoon and climate during the last glacial interglacial period (0-140,000 years): mineralogy and geochemistry of ODP Sites 1143 and 1144, South China Sea. Mar. Geol. 201, doi:S0025-3227(03)00214-7, this issue.

Tan, Z., Wang, Y., 1992. Distribution of clay minerals in the northern South China Sea (in Chinese). Acta Oceanol. Sin. 14, 64–71.

Thiry, M., 2000. Palaeoclimatic interpretation of clay minerals in marine deposits: an outlook from the continental origin. Earth Sci. Rev. 49, 201–221.

Thompson, P.R., Bé, A.W.H., Duplessy, J.C., Shackleton, N.J., 1979. Disappearance of pink-pigmented *Globigerinoides ruber* at 120,000 yr B.P. in the Indian and Pacific Oceans. Nature 280, 554–558.

Trentesaux, A., Liu, Z., Colin, C., Clemens, S.C., Boulay, S., Wang, P., 2003. Pleistocene paleoclimatic cyclicity of southern China: clay mineral evidence recorded in the South China Sea (ODP Site 1146). In: Prell, W.L., Wang, P., Blum, P., Clemens, S. (Eds.), Proc. ODP Sci. Res., Vol. 184, 1–10 (online).

Wang, L., Sarnthein, M., Erlenkeuser, H., Grimalt, J., Grootes, P., Heilig, S., Ivanova, E., Kienast, M., Pelejero, C., Pflaumann, U., 1999. East Asian monsoon climate during the Late Pleistocene: high-resolution sediment records from the South China Sea. Mar. Geol. 156, 245–284.

Wang, P., Prell, W.L., Blum, P., et al. (Eds.), 2000. Proc. ODP Init. Rep., Vol. 184 [CD-ROM]. Available from: Ocean Drilling Program, Texas A&M University, College Station, TX 77845-9547, USA.

Wang, P., Wang, L., Bian, Y., Jian, Z., 1995. Late Quaternary paleoceanography of the South China Sea: surface circulation and carbonate cycles. Mar. Geol. 127, 145–165.

Wang, Y., Zhang, Z., Huang, W., Gu, J., 1995. Hydrochemical characteristics and clay minerals of suspended sediment in south channel, Changjiang Estuary (in Chinese, with English abstr.). Mar. Sci. Bull. 14, 106–113.

Webster, P.J., 1994. The role of hydrological processes in ocean-atmosphere interactions. Rev. Geophys. 32, 427–476.

Xiao, J., An, Z., 1999. Three large shifts in East Asian monsoon circulation indicated by loess-paleosol sequences in China and late Cenozoic deposits in Japan. Palaeogeogr. Palaeoclimatol. Palaeoecol. 154, 179–189.

Xu, Y., Zhu, Z., Wen, Q., Wen, G., Pu, Z., 1999. Clay mineral, chemical characteristics and environmental record of the multi-stage laterite at Yingfengling Section, Leizhou Peninsula (in Chinese, with English abstr.). Geochimica 28, 281–288.

You, Z., Tang, J., Liao, L., 1993. Study on clay mineral in sediment cores from western Taiwan Strait (in Chinese, with English abstr.). J. Oceanogr. Taiwan Strait 12, 1–7.